Modelling of Ground Water Transport on Ancient Mars

F. Chaffard[1,2], **A. Kamada**[1,3], **T. Kuroda**[1], and **N. Terada**[1], [1]*Department of Geophysics, Graduate School of Science, Tohoku University, Sendai, Japan,* [2]*Physics Department, École Normale Supérieure – PSL, Paris, France (francois.chaffard@ens.psl.eu),* [3]*Earth-Life Science Institute, Institute of Science Tokyo, Tokyo, Japan.*

Introduction:

Over the past few decades, substantial geological evidence, such as outflow channels [1], valley networks [2], deltas [3], and ancient lakebeds [4], has accumulated indicating the presence of an active hydrological cycle on early Mars. Those features suggest that liquid water once played an active role in shaping the Martian surface. However, the origin of liquid water and mechanisms for the formations of those features remain debated, with hypotheses such as liquid precipitation-driven erosion [5], basal melting of ice sheets [6], groundwater upwelling [7], and catastrophic flooding events [8].

As for the former two hypotheses, investigations using numerical climate and hydrological models have been made [9-13]. Our group have developed a coupled Paleo-Mars Global Climate Model (PMGCM) [14] with surface river transport (CRIS: Catchment-based RIver Simulater) [15] and ice sheet evolution (ALICE: Accumulation and ablation of Large-scale ICE-sheets with dynamics and thermodynamics) [16], which reproduced the surface outflow equivalent to the formation of observed valley networks [17] by precipitation and/or basal melting depending on the climate scenario (warm or cool).

Focusing on the groundwater upwelling, there are signs of deep aquifers and groundwater resurgence, particularly in northern equatorial basins such as Arabia Terra and Meridiani Planum [7,12]. These regions not only show morphological signs of past groundwater activity but also host mineralogical evidence—such as hematite "blueberries"—indicative of prolonged water-rock interaction [18]. Reproducing numerically groundwater upwelling in these regions could help to validate or invalidate certain climatic scenarios, but because horizontal groundwater transport is such a long time scale mechanism, it has not been included in most works. A preceding study [13] used a 2D horizontal approximation of groundwater transport to compute very large time scale evolution of the water table and successfully obtained groundwater upwelling in Meridiani Planum region. That model only computed horizontal groundwater transport using a preset low latitude precipitation belt as instant aquifer recharge, not accounting for potential presence of ice.

Now we are implementing a three-dimensional, planetary-scale model of groundwater evolution tailored to early Martian conditions coupled with our PMGCM [14-16]. Here we show preliminary results of our ground water transport model with forced precipitation taken from the PMGCM model output. With the coupled model, we are aiming to explore where and under what conditions groundwater upwelling might have occurred—and what that implies for the Martian water cycle and possible climatic scenarios.

Method:

The three-dimensional groundwater transport model is based on [19]. It solves at each time step the mixed form Richards equation using a finite volume scheme, fully implicit time stepping and total head as primary variable:

$$\frac{\partial \theta}{\partial t} + S_s S_w \frac{\partial h}{\partial t} = \nabla(K(h)\nabla h) + Q$$

where θ is moisture content [kg m^{-3}], $h = \psi + z$ is total hydraulic head [m], ψ is pressure head [m], z is elevation head [m], S_s is specific storage [m^{-1}], K is hydraulic conductivity [m s^{-1}], S_w is 0 for unsaturated layers and 1 otherwise, and Q is water source [s^{-1}]. Moisture and conductivity functions ($\theta(h)$ and $K(h)$) are taken from the Van Genuchten - Mualem model. Nonlinearities of the discretized equation are solved with an inexact Newton method, the convergence criteria is:

$$max_i \left| h_i^{m+1,k+1} - h_i^{m+1,k} \right| < \epsilon$$

where i denotes layer, m denotes time step, k is iteration step, and ϵ is an arbitrary threshold taken here to be 10^{-5}.

The horizontal resolution of the model is set to ~5.6° for both in latitude and longitude (fitting to T21 resolution of our PMGCM), and the precipitation data driving surface boundary condition is taken from a run of the PMGCM assuming the surface pressure of 2 bar, obliquity of 40°, and H_2 mixing ratio of 6% (warm scenario) [15]. The vertical domain is divided into 29 layers. The thickness of the top ground layer is 5 mm, and the lower boundary condition is set to be no transport below bedrock, whose depth is 10 km.

For now, parameters like moisture saturation limit θ_s and saturated conductivity K_s are set as constant along depth, but we could change that in the future using for example models described in [20]. At the initial condition, any layer located below -2.3 km of elevation with respect to datum (which was set to be the ocean shoreline in the PMGCM) is saturated so that there is a globally equal total head. The time step of calculation is set to 100 Mars Years (MYs).

Results and Discussions:

The simulation reached equilibrium in ~3×10^5 MYs, as shown in Figure 1.

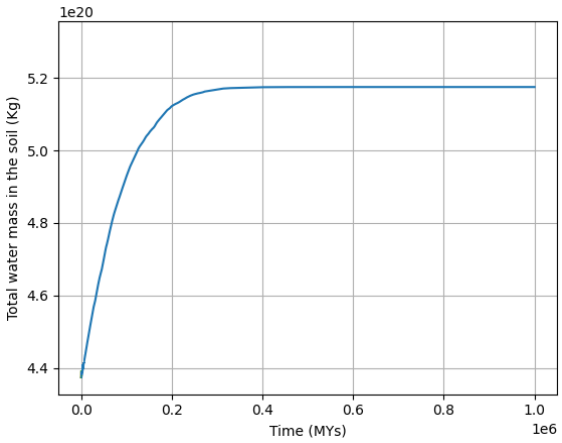

Figure 1: Total water mass in the soil evolution.

Figures 2-4 show the moisture content in the surface soil layer at the initial condition, after 10^5 MYs calculation, and after 10^6 MYs calculation (equilibrium state), respectively. Initial condition shows the northern ocean and Hellas bassin as fully saturated water columns (Figure 2). The regions where the water table reaches the surface quickly (within 10^5 MYs) are Arabia Terra, and south of Elysium Montes in continuity with the initial ocean (Figure 3). At equilibrium the water table reached the surface in several other localized regions, mostly in the southern highlands, even near Tharsis region (Figure 4).

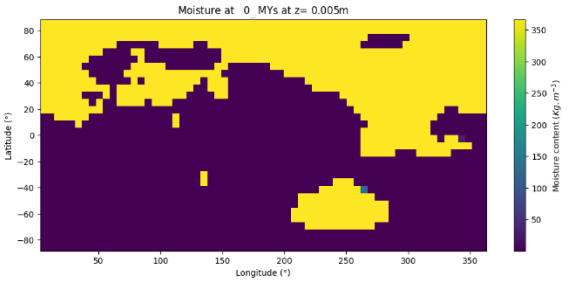

Figure 2: Moisture content in the surface soil layer at the initial condition.

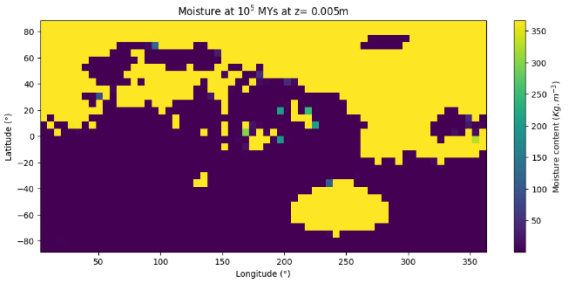

Figure 3: Same as Figure 2 but after 10^5 MYs calculation.

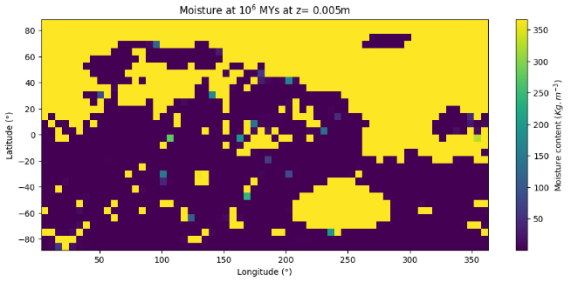

Figure 4: Same as Figure 2 but after 10^6 MYs calculation.

As far as we know, geological evidence of groundwater upwelling has not been found in those regions, so it may indicate that we overestimate initial available water in our model. First, the saturation limit θ_s is thought to decrease sharply with depth [20], so setting it constant overestimates water inventory and horizontal groundwater transport in the deepest layers that can ultimately lead to upwelling. Also, we set the ocean shoreline to -2.3 km but this value is quite uncertain while being the main driver of water inventory. Actually, most geological features tend towards a shoreline located deeper around -4 to -5 km [7,21], but the precipitation computations of the PMGCM were done with a higher standing ocean so we kept the PMGCM value for coherence.

Nonetheless, the model successfully predicts groundwater upwelling in Arabia Terra and in other northern equatorial regions where geological evidence of resurgence has been found. As water table reached the surface faster in those regions than in the Southern highlands, we can expect that it would still happen at equilibrium even if we lower the total water inventory.

To investigate further there are many things that should be done. First, we would try new parameters of total water inventory (ocean shoreline and saturation limit values). Then, we would also try a high spatial resolution run to compare in detail with basins where the water table is thought to have reached the surface, in particular in the northern equatorial region. The final goal of the development would be to fully couple the model to the PMGCM.

References:

[1] Baker, V.R. (1982), The Channels of Mars, University of Texas Press.

[2] Carr, M.H. (1995), The Martian drainage system and the origin of valley networks and fretted channels, *Journal of Geophysical Research: Planets*, 100(E4), 7479–7507.

[3] Goudge, T.A. et al. (2015), Insights into surface runoff on early Mars from paleolake basin morphology and stratigraphy, *Journal of Geophysical Research: Planets*, 120(4), 775–808.

[4] Fassett, C.I. & Head, J.W. (2008), Valley network-fed, open-basin lakes on Mars: Distribution and implications for Noachian surface and subsurface hydrology. *Icarus*, 198(1), 37–56.

[5] Craddock, R.A. & Howard, A.D. (2002), The case for rainfall on a warm, wet early Mars, *Journal of Geophysical Research: Planets*, 107(E11), 5111, 2002.
[6] Galofre, A.G. et al. (2020), Valley formation on early Mars by sub 3 glacial and fluvial erosion, *Nature Geoscience*, 13 (10), 663–668.
[7] Salese, F. et al. (2019), Geological Evidence of Planet-Wide Groundwater System on Mars, *Journal of Geophysical Research. Planets*, 124(2), 374–395.
[8] Carr, M.H. (1979), Formation of Martian flood fea tures by release of water from confined aquifers, *Journal of Geophysical Research: Solid Earth*, 84(B6), 2995–3007.
[9] Wordsworth, R. et al. (2013), Global modelling of the early martian climate under a denser CO_2 atmosphere: Water cycle and ice evolution, *Icarus*, 222(1), 1–19.
[10] Ramirez, R.M. (2017), A warmer and wetter solution for early Mars and the challenges with transient warming, *Icarus*, 297, 71–82.
[11] Turbet, M. & and Forget, F. (2021), 3-D Global mod elling of the early martian climate under a dense CO_2+H_2 atmosphere and for a wide range of sur face water inventories, arXiv:2103.10301.
[12] Andrews-Hanna, J.C. et al. (2010). Early Mars hydrology: Meridiani playa deposits and the sedimentary record of Arabia Terra, *Journal of Geophysical Research: Planets*, 115(E6), E06002.
[13] Andrews-Hanna, J.C. & Lewis, K.W. (2011), Early Mars hydrology: 2. Hydrological evolution in the Noachian and Hesperian epochs. *Journal of Geophysical Research: Planets*, 116(E2), E02007.
[14] Kamada, A. et al. (2020), A coupled atmosphere-hydrosphere global climate model of early Mars: a 'cool and wet' scenario for the formation of water channel, *Icarus*, 338, 113567.
[15] Kamada, A. et al. (2021), Global climate and river transport simulations of early Mars around the Noachian and Hesperian boundary, *Icarus*, 368, 114618.
[16] Kamada, A. et al. (2022), Evolution of ice sheets on early Mars with subglacial river systems, *Icarus*, 385, 115117.
[17] Hynek, B.M. et al. (2010), Updated global map of Martian valley networks and implications for climate and hydrologic processes, *Journal of Geophysical Research: Planets*, 115(E9), E09008.
[18] Squyres, S.W. et al. (2004), In situ evidence for an ancient aqueous environment at Meridiani Planum, Mars, *Science*, 306(5702), 1709–1714.
[19] Miura, Y. and Yoshimura, K. (2020), Development and Verification of a Three-Dimensional Variably Satu rated Flow Model for Assessment of Future Global Water Resources, *Journal of Advances in Modeling Earth Systems*, 12(8), e2020MS002093.
[20] Hanna, J.C. & Phillips, R.J. (2005), Hydrologi cal modeling of the Martian crust with application to the pressurization of aquifers. *Journal of Geophysical Research: Planets*, 110(E1), E01004.
[21] Sholes, S.F. et al. (2021), Where are Mars' Hypothesized Ocean Shorelines? Large Lateral and Topographic Offsets Between Different Versions of Paleoshoreline Maps. *Journal of Geophysical Research: Planets*, 126(5), e2020JE006486.